Royal Netherlands
Meteorological Institute
Ministry of Infrastructure
and Water Management

PGV levels and location uncertainty for the Winde events in August 2023

E. Ruigrok, P. Kruiver

De Bilt, 2023 | Technical report; TR 410

Royal Netherlands
Meteorological Institute
Ministry of Infrastructure
and Water Management

PGV levels and location uncertainty for the Winde events in August 2023

KNMI, R&D Seismology and Acoustics

October 14, 2023

Introduction

In August, 2023, two events occurred in the village of Winde in Drenthe; the first earthquake at 22-08-2023 18:39:08.69 UTC with a local magnitude of 1.56, the second earthquake at at 23-08-2023 12:05:48.6 UTC with a local magnitude of 1.71. Both events were detected by the KNMI network (*KNMI*, 1993) and located near-real time with the Hypocenter method (*Lienert et al.*, 1986). These fast solutions use an average 1D model for the north of the Netherlands (*Kraaijpoel and Dost*, 2013). In this report, updated epicenters and their uncertainties are listed. Moreover, peak-ground velocity (PGV) levels are extracted from the recordings. These are used, together with a ground motion prediction equation, to find out whether it is likely that PGV levels occurred of 2 mm/s and higher.

Epicenters

The epicenters are improved by using a best-fitting traveltime versus distance model based on a database of local P-wave traveltime picks. This data-driven model incorporates actual underburden velocities and only well pickable phase arrivals. An error estimate is derived from the spread in picking times from the best-fitting model. This error incorporates both the local variations of the velocity field as well as picking errors. These errors are propagated further into epicentral probability density functions (PDFs). This results into updated epicenters and their 95% confidence regions. Details of the method are described in *Ruigrok et al.* (2023).

Figs. 1 and 3 show the seismic sensors where manual P-wave picks are available for the two Winde events. A grid search is performed for a region around the Hypocenter solution, as indicated by the red boxes in the figures. In the first step, equal differential time (EDT, *Zhou*, 1994) residuals are computed. That is, for each grid point and for each station combination, the traveltime differences are forward modelled and tabulated. From these values, the observed traveltime differences are subtracted to obtain the EDT residuals. In the second step, the PDF is derived from the EDT residuals, using a L1 norm (*Tarantola*, 2005). Figs. 2 and 4 show the 95% confidence areas of the resulting PDFs. The locations with the maximum probability are assigned to be the updated epicenters.

August 22, 2023

The following list contains the new epicenter for the Winde 22-08-2023 event, both in wgs84 coordinates and in the Dutch national triangulation system (RD). The line that surrounds the 95% confidence zone is by approximation an ellipse. The parameters of this ellipse (major axis, minor axis and orientation) are listed, together with the standard deviations describing the epicentral PDF in the direction with the largest uncertainty σ_1 and the perpendicular direction with the smallest uncertainty σ_2.

Epicenter in wgs84 [deg]: 6.4969, 53.1157
Epicenter in RD [m]: 229300, 570450
Ellipse major and minor axes [m]: 992, 670
σ_1 and σ_2 [m]: 203, 137
Orientation of the major axis [deg]: 150

The waveform data used in the above analysis is publicly available and can be obtained through:

GUI: `http://rdsa.knmi.nl/dataportal/`

FDSN webservices: `http://rdsa.knmi.nl/fdsnws/dataselect/1/`

August 23, 2023

The following list contains the new epicenter for the Winde 23-08-2023 event, both in wgs84 coordinates and in the Dutch national triangulation system (RD). The line that surrounds the 95% confidence zone is by approximation an ellipse. The parameters of this ellipse (major axis, minor axis and orientation) are listed, together with the standard deviations describing the epicentral PDF in the direction with the largest uncertainty σ_1 and the perpendicular direction with the smallest uncertainty σ_2.

Epicenter in wgs84 [deg]: 6.4970, 53.1170
Epicenter in RD [m]: 229300, 570600
Ellipse major and minor axes [m]: 648, 510
σ_1 and σ_2 [m]: 132, 104
Orientation of the major axis [deg]: 115

PGV levels

For induced events outside Groningen, the protocol as established in *Ruigrok and Dost* (2020a) is used to compute PGV[1] contours. From the spatial distribution of PGV, contours are extracted for the P50, P90 and P99 probabilities. The P50 is the average field, which thus has a 50% probability of exceedance. The P90 is the 90th percentile, which PGV field has a 10% probability of exceedance. The P99 has a 1% probability of exceedance.

The PGV field is a combination of a model and local recordings. The model BMR2 (*Ruigrok and Dost*, 2020a) is used. This is a ground motion prediction equation that provides the PGV level and its variability as a function of magnitude, epicentral distance and depth of the event. The model has been calibrated with PGV recordings from induced events in the Netherlands. Recordings at the Earth's surface from one specific event are used to estimate how much stronger, or weaker, this event is with respect to the average event in the database. This yields the so-called event term, which is used to adapt the model with a distance-independent shift up, or downwards. Still, uncertainty exists of the actual PGV that materialized at a certain location. This so-called within-event variability is caused, e.g., by the radiation pattern of the source and variations in near-surface amplification. At and nearby places where the PGV has been recorded, the uncertainty of the PGV is reduced by blending the model with the actually measured PGV.

[1] In this report, as PGV measure we use 'PGVrot', which is defined as $max(\sqrt{u_E^2(t) + u_N^2(t)})$, where $u_E(t)$ and $u_N(t)$ are the particle-velocity recording on the East and North component, respectively.

If the combined field reaches levels of 2 mm/s and higher, PGV contours are extracted and shown on a map.

August 22, 2023

For the Winde 22-08-2023 event, all accelerometer recordings at distances smaller than 30 km are evaluated, which yields 18 recordings with a signal-to-noise ratio larger or equal to 6 dB. The nearest and furthest accepted stations are at 1.61 and 24.89 km epicentral distance, respectively. Table 1 lists the PGV values. Fig. 5 shows these recorded PGV values as function of epicentral distance, together with the event-term shifted BMR2 model for M=1.56. As hypocenter depth, 3.3 km is taken. It is assumed that the current Winde event has the same nucleation depth as the one of 27-09-2020 (*Ruigrok and Dost*, 2020b).

Using the 18 recordings results in an event term of 0.0597. This is the average difference between modeled and recorded PGV levels (expressed in natural log). With the event term quantified, the remaining model variability is the within-event variability $\phi = 0.536$. This remaining variability is implemented to yield the confidence regions as plotted in Fig. 5 (dashed grey lines). This figure shows that even the P99 field does not reach the minimum threshold PGV value of 2 mm/s. Hence, no PGV contours are drawn on a map for this event.

Station name	**Epicentral distance [km]**	**PGV [mm/s]**
N010	1.61	0.313
DON	3.51	0.148
N020	5.68	0.122
G660	9.22	0.020
G380	10.02	0.042
VRS	11.41	0.008
ASS2	12.31	0.034
ZDL	14.33	0.015
G690	14.58	0.032
G440	15.89	0.022
ASS1	15.86	0.028
G490	16.99	0.028
GK040	18.45	0.015
G260	18.79	0.028
G390	19.44	0.012
BFB2	19.61	0.010
G340	23.48	0.011
G160	24.89	0.014

Table 1: Recorded PGVs for the Winde 22-08-23 event

August 23, 2023

For the Winde 23-08-2023 event, all accelerometer recordings at distances smaller than 30 km are evaluated, which yields 20 recordings with a signal-to-noise ratio larger or equal to 6 dB. The nearest and furthest accepted stations are at 1.59 and 27.48 km epicentral distance, respectively. Table 2 lists the PGV values. Fig. 6 shows these recorded PGV values as function of epicentral distance, together with the event-term shifted BMR2 model for M=1.71. As hypocenter depth, 3.3 km is taken.

Using the 20 recordings results in an event term of 0.1324. This is the average difference between modeled and recorded PGV levels (expressed in natural log). With the event term quantified, the remaining model variability is the within-event variability $\phi = 0.536$. This remaining variability is implemented to yield the confidence regions as plotted in Fig. 6. This figure shows that only the P99 field reaches the minimum threshold PGV value of 2 mm/s.

The modeled PGV fields (Fig. 6) are locally corrected with the recorded PGV levels (Table 2). This results in a maximum PGV of 1.37 mm/s in the P99 field. Since this value is lower than 2 mm/s, no contour is drawn on the map for this earthquake.

Station name	**Epicentral distance [km]**	**PGV [mm/s]**
N010	1.59	0.470
DON	3.58	0.185
N020	5.81	0.223
G660	9.10	0.035
G380	9.88	0.063
ASS2	12.44	0.017
G720	14.42	0.032
ZDL	14.37	0.025
G690	14.47	0.043
BRTL	15.13	0.058
G440	15.80	0.036
ASS1	16.01	0.050
G490	16.93	0.033
G540	17.44	0.017
GK040	18.34	0.024
G260	18.64	0.018
G390	19.35	0.020
BFB2	19.55	0.016
EVK	21.42	0.019
DR030	27.48	0.016

Table 2: Recorded PGVs for the Winde 23-08-23 event

Discussion and Conclusions

In August 2023 two events occured in the village Winde in Drenthe. The locations of the M1.6 and M1.7 events are at the northern edge of the Vries-North gas field (Figs 2 and 4). In this area, two times before there has been a sequence of two events within two days. The first sequence was in December 1996 (Bunne M1.9 and Bunne M1.8) about 1 km southeast of the events described in this report. The second sequence was in September 2020 (Winde M0.9 and Winde M1.8) about 500 m north of the events described in this report, at the southern edge of the Roden gas field. *Ruigrok and Dost* (2020b) analyzed the location and ground motions of the Winde M1.8 event. *NAM* (2020) investigated the underlying cause of the Winde M0.9 and M1.8 events. The most likely cause was pressure depletion through water migration. Water is flowing from the acquifer between the Roden and Vries gas fields into the largely depleted Vries gas field. This water flow causes a pressure depletion in the source area, resulting in stressing of the existing faults that bound a transitional block between the Roden and Vries gas fields. The August 2023 events are located at the southern edge of the transitional block. It is likely that also these events are caused by water drainage from the transitional block into the Vries gas field.

For the Winde 22-08-23 event, the highest recorded PGV is 0.313 mm/s at station N010. For the Winde 23-08-23 event, the highest PGV is 0.470 mm/s, also recorded at station N010. For this second event, a ground-motion prediction equation and the measured PGV values have been used to compute the PGV field that has a 1% chance of exceedance. This P99 PGV field reaches a maximum of 1.37 mm/s at the epicenter.

References

KNMI (1993), Netherlands Seismic and Acoustic Network, Royal Netherlands Meteorological Institute (KNMI), Other/Seismic Network, doi:10.21944/e970fd34-23b9-3411-b366-e4f72877d2c5.

Kraaijpoel, D., and B. Dost (2013), Implications of salt-related propagation and mode conversion effects on the analysis of induced seismicity, *Journal of Seismology*, *17*(1), 95–107.

Lienert, B. R., E. Berg, and L. N. Frazer (1986), HYPOCENTER: An earthquake location method using centered, scaled, and adaptively damped least squares, *Bulletin of the Seismological Society of America*, *76*(3), 771–783.

NAM (2020), Winde bevingen, 26 en 27 september 2020, *NAM-report: EP202010200882*, `https://www.nam.nl/news/2020/reporting-quakes-winde-drenthe/_jcr_content/root/main/section_top/section_main/text.multi.stream/1685114906849/2a91483b1ee71c540414dda976254f4a8c351af0/winde-quakes-27-9-2020-nam-reporting.pdf`.

Ruigrok, E., and B. Dost (2020a), Advice on the computation of peak-ground-velocity confidence regions for events in gas fields other than the Groningen gas field, *KNMI Technical Report*, *TR-386*.

Ruigrok, E., and B. Dost (2020b), PGV levels and location uncertainty for the Winde 27-09-2020 event, *KNMI Technical Report*, *TR-388*.

Ruigrok, E., P. Kruiver, and B. Dost (2023), Construction of earthquake location uncertainty maps for the Netherlands, *KNMI Technical Report*, *TR-405*.

Tarantola, A. (2005), *Inverse Problem Theory and Methods for Model Parameter Estimation*, SIAM, Philadelphia.

Zhou, H.-w. (1994), Rapid three-dimensional hypocentral determination using a master station method, *Journal of Geophysical Research: Solid Earth*, *99*(B8), 15,439–15,455.

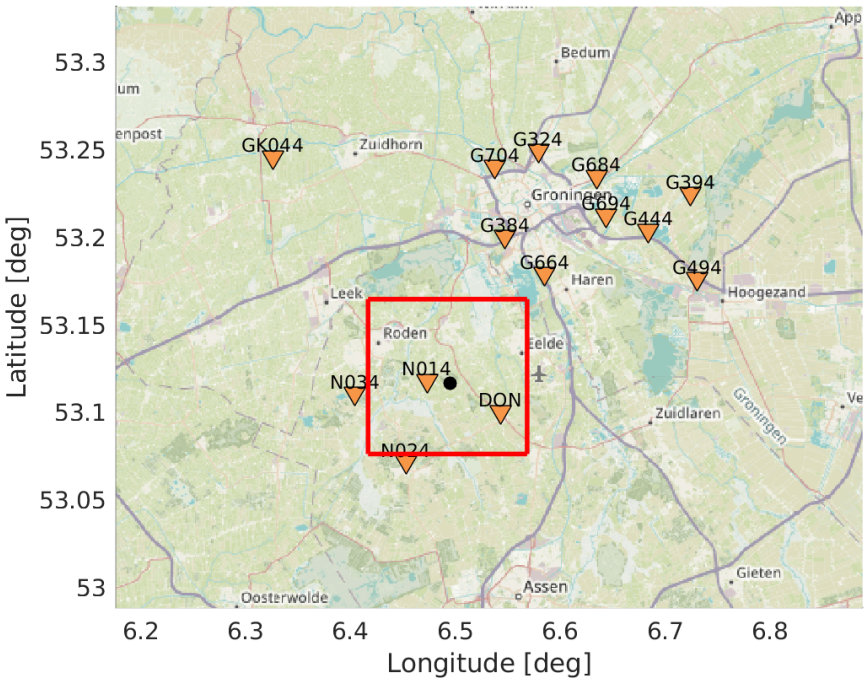

Figure 1: Overview map for the Winde 22-08-2023 event with locations of stations (orange triangles) where P-wave onsets were picked, the fast Hypocenter solution (black dot) and the boundary line of the area in which a grid search is done (red box). Background map is from www.openstreetmap.org.

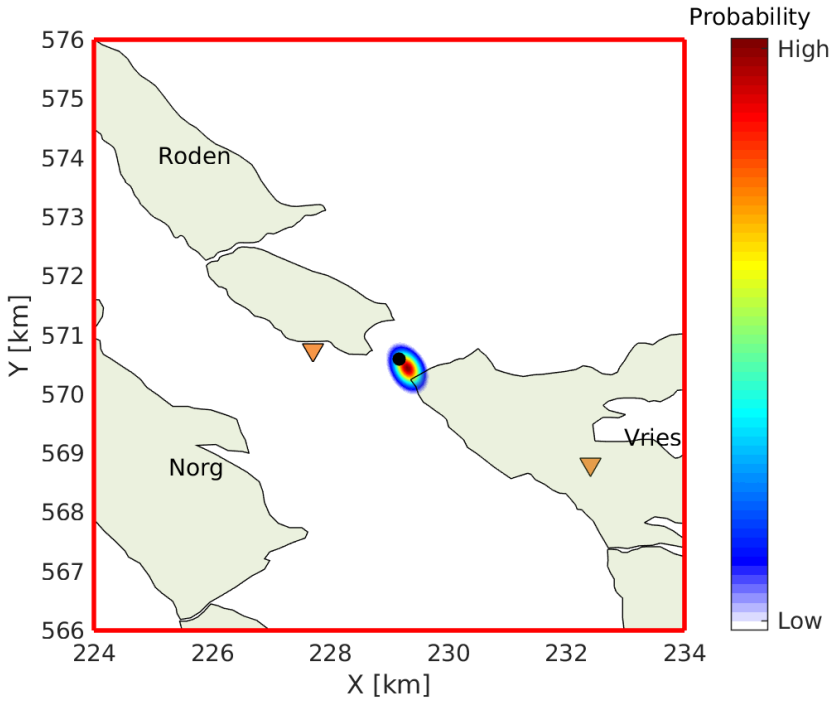

Figure 2: Map showing hydrocarbon fields (green-filled polygons), the fast Hypocenter solution (black dot) and the epicentral probability density function (PDF) of the Winde 22-08-2023 event using time-differences and an optimized model. The coloured area is the 95% confidence zone of the PDF. The field polygons are from www.nlog.nl, using the March 2020 update.

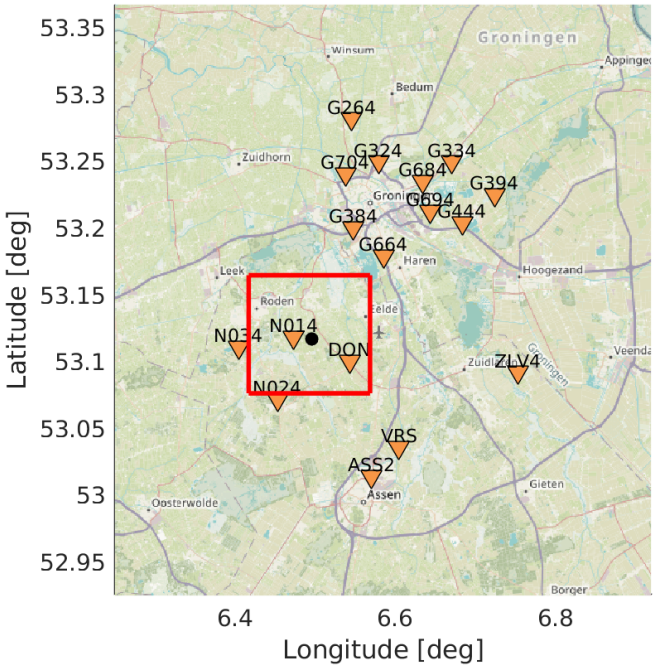

Figure 3: Overview map for the Winde 23-08-2023 event with locations of stations (orange triangles) where P-wave onsets were picked, the fast Hypocenter solution (black dot) and the boundary line of the area in which a grid search is done (red box). Background map is from www.openstreetmap.org.

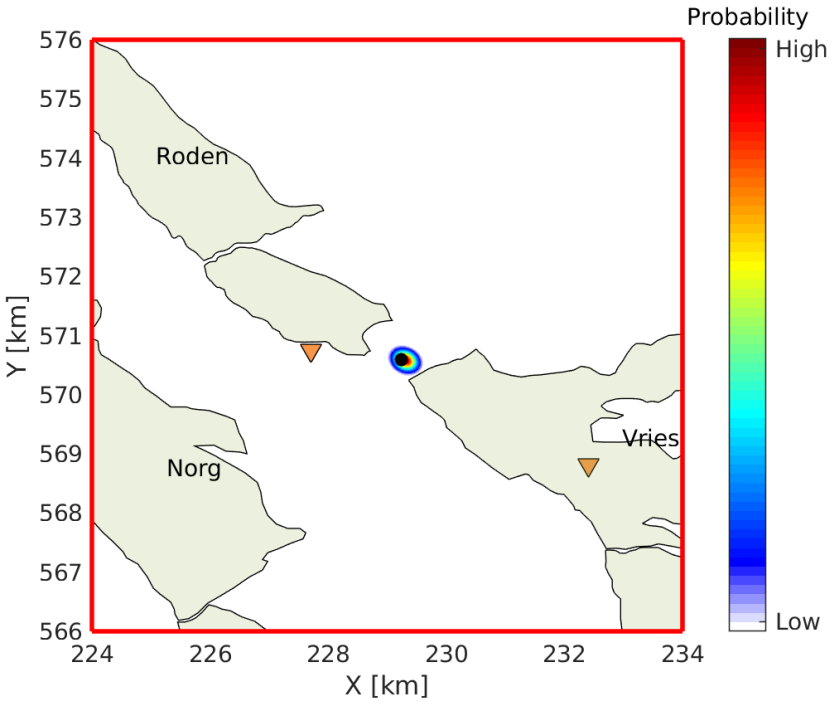

Figure 4: Map showing hydrocarbon fields (green-filled polygons), the fast Hypocenter solution (black dot) and the epicentral probability density function (PDF) of the Winde 23-08-2023 event using time-differences and an optimized model. The coloured area is the 95% confidence zone of the PDF. The field polygons are from www.nlog.nl, using the March 2020 update.

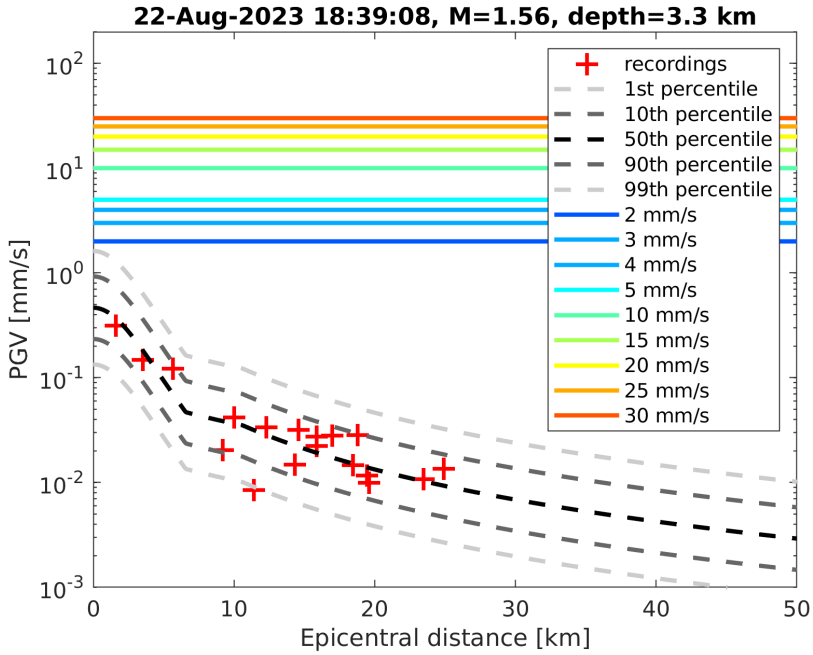

Figure 5: BMR2 model and confidence regions for this model (dashed lines), PGV thresholds (coloured lines) and measured PGV values for the Winde event (red crosses). Both the model and the recordings are expressed in PGVrot.

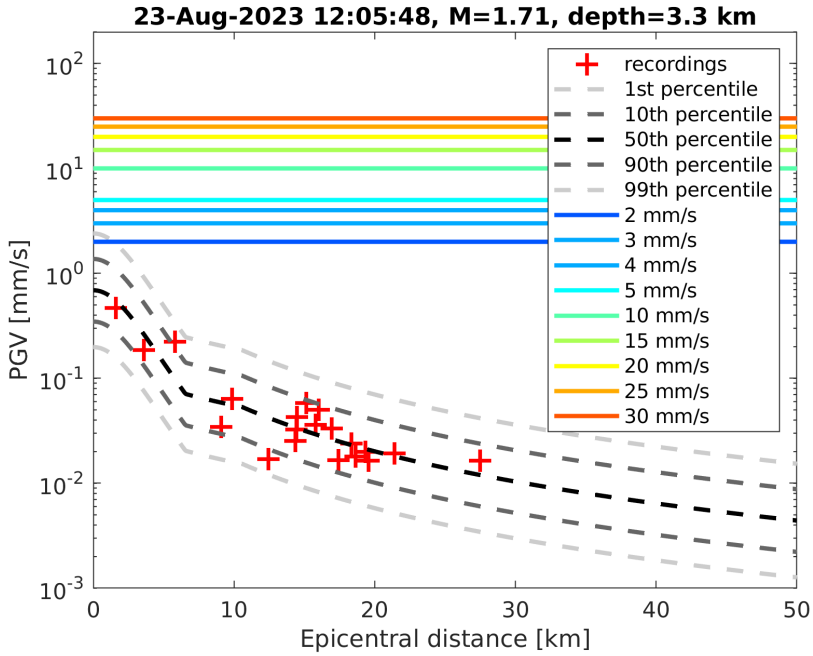

Figure 6: BMR2 model and confidence regions for this model (dashed lines), PGV thresholds (coloured lines) and measured PGV values for the Winde event (red crosses). Both the model and the recordings are expressed in PGVrot.

Royal Netherlands Meteorological Institute

PO Box 201 | NL-3730 AE De Bilt
Netherlands | www.knmi.nl